2.3 SEM AND EBSD CHARACTERIZATION OF Fe - {110} $Y_2Ti_2O_7$ INTERFACES – T. Stan, Y. Wu, G. R. Odette (University of California Santa Barbara)

OBJECTIVE

The objective of this work is to create mesoscopic scale interfaces which help further understand the role of Y-Ti-O nano-features in the bcc Fe-Cr ferrite matrix found in nanostructured ferritic alloys (NFAs).

SUMMARY

Nanostructured ferritic alloys (NFAs) are dispersion strengthened by a high density of 2-3 nm fcc pyrochlore $Y_2Ti_2O_7$ nano features (NFs). The interface between the bcc ferrite matrix and the $Y_2Ti_2O_7$ plays critical role in the radiation damage resistance of NFAs. However, details about the interfaces are difficult to determine from the nm-scale features themselves. To partially overcome this obstacle, and to complement other characterization studies of the actual NFs themselves, mesoscopic interfaces were created by electron beam deposition of Fe onto {110} oriented $Y_2Ti_2O_7$ bulk single crystal surfaces. We report characterization of Fe – {110} $Y_2Ti_2O_7$ interfaces using the Scanning Electron Microscopy (SEM) and Electron Backscatter Diffraction (EBSD) techniques. The polycrystalline Fe films had grains with three distinct orientation relationships (ORs). Notably, one 10 μm Fe grain had the favored {100}Fe||{110}$Y_2Ti_2O_7$ and <100>Fe||<100>$Y_2Ti_2O_7$ OR which is found in matrix embedded NFs. This work is continuing and while the mesoscopic interfaces may differ from those of the embedded NFs, the former will facilitate characterization of controlled interfaces, such as interactions with point defects and helium.

BACKGROUND

Materials in fusion reactor environments are subject to intense radiation fields, large time-varying stresses, high temperatures, and chemically reactive environments [1]. Transmutation reactions produce helium (He) which interacts with displacement damage to drive complex microstructural evolutions. Notably, He precipitates as gas bubbles which help nucleate growing voids and creep cavities, and embrittle grain boundaries. Nanostructured Ferritic Alloys (NFAs) are radiation tolerant due to the ultrahigh density of Y-Ti-O nanofeatures (NFs) which trap He in harmless fine-scale bubbles that suppress void swelling and embrittlement. The interface between the matrix and NFs also act as sinks for defect annihilation and provide high creep strength due to dislocation pinning [2].

Numerous Transmission Electron Microscopy (TEM) studies have shown that NFs are complex oxides, primarily fcc cubic pyrochlore $Y_2Ti_2O_7$ [3-8]. Wu et al. reported a comprehensive TEM characterization study of an NFA variant (MA957) in different conditions, using various techniques [9]. The work showed that extracted NFs are structurally consistent with $Y_2Ti_2O_7$ and are generally near stoichiometric with Y/Ti ratios from 0.5 to 1. The dominant in-foil interface was found to be parallel to the {100} planes in Fe, although the oxides themselves could not be indexed due to their small size (≈ 2 nm). This paper also discusses some other work in the literature that did not find the pyrochlore $Y_2Ti_2O_7$. Henceforth, $Y_2Ti_2O_7$ will be referred to as YTO.

A study by Ribis et al. on 1100°C annealed Fe-Cr-W-Y-Ti-O alloys reported ≈ 10 nm YTO type NFs [10]. The orientation relationships (ORs) between these NFs and the matrix are: {100}Fe||{100}YTO and <100>Fe||<100>YTO. Finally, a high resolution TEM (HRTEM) study by Cisten et al. confirmed that the

in-foil NF in the same friction stirred weld variant of MA957 are $Y_2Ti_2O_7$ [11]. This study using TEAM 0.5 HRTEM showed that the dominant NF in-foil interface OR is {100}Fe||{100}YTO and <100>Fe||<110>YTO. This OR is different from the one found by Ribis et al. by a 45 degree bulk rotation of the oxide within the matrix. The observations by Ciston et al. indicate that the NFs have two interfacial ORs. The first happens to be the same as the bulk OR: {100}Fe||{100}YTO and <100>Fe||<110>YTO. The second is: {100}Fe||{110}YTO and <100>Fe||<100>YTO.

NFs embedded in a matrix are difficult to study due to their small size, of order 2-3 nm. Thus larger scale interfaces were created by electron beam deposition of Fe onto oriented YTO single crystal surfaces. Preliminary studies on {111} YTO surfaces show that the character of the Fe film is affected by the YTO surface crystallographic orientation, YTO surface topology, and Fe deposition rate [12]. This work has now been extended to {110} YTO surfaces. While these interfaces may differ from those for embedded NFs, creating a variety of mesoscopic surrogates with self-selected ORs will facilitate developing an understanding of metal-oxide interfaces in NFAs, especially with respect to their structures and functional properties.

PROGRESS AND STATUS

Experimental Methods

The details of how samples were fabricated and what instruments were used for characterization are covered in a previous publication [12] and a Fusion Semiannual Report [13]. In summary, a pure single crystal of $Y_2Ti_2O_7$ was {110} oriented and a 2 mm thick wafer was cut using a wire saw. An Allied Multi-prep instrument was used to polish the wafer using a sequence of diamond lapping films, followed by a final 15 minute polishing step using a 0.02 µm non-crystallizing silica suspension. An electron beam system was used to deposit Fe on the $Y_2Ti_2O_7$ crystal at 6.2×10^{-6} torr and 800°C. The deposition rate was 8 nm/s for 250 s, producing an Fe layer thickness of ≈ 2 µm. The sample was then cooled to room temperature at a rate of ≈ 0.16°C/s.

Results and Discussion

<u>Scanning Electron Microscope (SEM) and Electron Backscatter Diffraction (EBSD) Characterization</u>

Figure 1(a) is a Scanning Electron Microscope (SEM) image taken from the Fe film on {110} $Y_2Ti_2O_7$. There are three types of surface topologies (marked 1, 2 and 3 on the figure). Area 1 is flat and has ripples and ridges across the surface. This area coalesced as one continuous film and did not have clear grain boundaries. However, there are some surface cracks in this area. About most of the $Y_2Ti_2O_7$ surface was covered by this kind of Fe film. The sample also has ≈ 2 µm pointed grains which are marked with 2 in Figure 1(a). Some of these grains were isolated within the cracks in the flat areas, while others were found in groups. These grains occupy about a very small fraction of the total area of the sample. The final topology is marked with 3 in Figure 1(a). This ≈ 10 µm grain is smooth and flat, and is the only one found on the entire sample. It is surrounded by both type 1 and type 2 Fe.

Figure 1(b) shows Electron Backscatter Diffraction (EBSD) data taken from the area marked by a green rectangle in Figure 1(a). Each out-of-plane crystallographic orientation of Fe is assigned a color based on the legend in the top right of Figure 1(b). Fe with an {100} surface orientation are marked with red, Fe with an {110} surface orientation are marked with green, Fe with a {111} surface orientation are marked with blue, and other orientations can be indexed using the legend. White areas in Figure 2(b) represent

locations where the crystallographic information could not be acquired. This is often due to interference from grain boundaries, rough surface topology, or surface contamination such as dust.

Figure 2(b) appears to show that area 1 has surface orientations marked with green and blue. However, further analysis (not shown) indicates that the blue parts were miss-indexed by the EBSD software and should be green. Thus, the large areas marked with 1 have the same out-of-plane orientation close to {110}. The peaked grains marked with 2 are all purple and have an orientation close to {112}. The large red grain marked with 3 is {100} oriented.

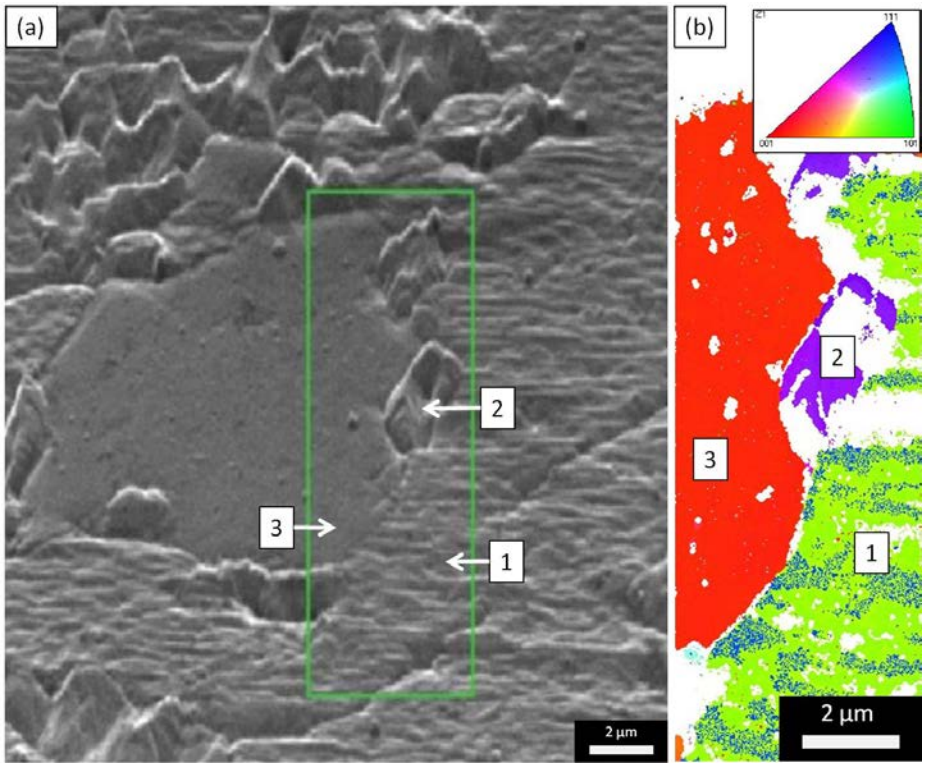

Figure 1. (a) An SEM image of the Fe film. Three surface topologies are marked by 1, 2, and 3. (b) EBSD image showing out-of-plane orientations of the Fe grains.

The EBSD data from Figure 1(b) is also represented as pole figures in Figure 2. Each part of Figure 2(a-d) shows the name of the material, four pole figures representing the 111, 110, 100, and 112 reflections, and a 3D cube showing the full crystallographic orientation. The green diamonds on the pole figures indicate the surface orientation, while the blue hexagons show the in-plane orientation. Figure 1(a) shows the crystallographic orientation of the YTO substrate. The green diamond in the center of the {110} pole figure and the accompanying 3D cube show that the substrate was {110} oriented.

Figure 2(b) shows EBSD data taken from the flat Fe film, referred to as area 1 in Figure 1. The film does not have a clear out-of-plane OR with the substrate. The Fe film likely has a high-index orientation close to {110}. By observing the overlap between the hexagons in the 100 Fe pole figure and the 110 YTO pole figure, the following in-plane OR is obtained: <100>Fe||<110>YTO.

Figure 2(c) shows EBSD data from the paked grains marked with 2 in Figure 1. These grains are clearly {112} surface oriented. By overlapping the diamonds and hexagons from the YTO substrate (Figure 2a) and those from the Fe grains (Figure 2c), the following OR is obtained: {112}Fe||{110}YTO and <111>Fe||<110>YTO. This OR has not been observed in any previous study on embedded NFs, nor on Fe depositions.

Figure 2(d) shows EBSD data from the large flat grain marked with 3 in Figure 1. The OR between this grain and the substrate is: {100}Fe||{110}YTO and <100>Fe||<100>YTO. Notably, this is one of the same ORs that was found in the study by Ciston et al. [11]. This result is significant since it shows that some surrogate interfaces can be created to have the same ORs as those found in embedded NFs. Further studies are required to show what fabrication conditions lead to specific ORs.

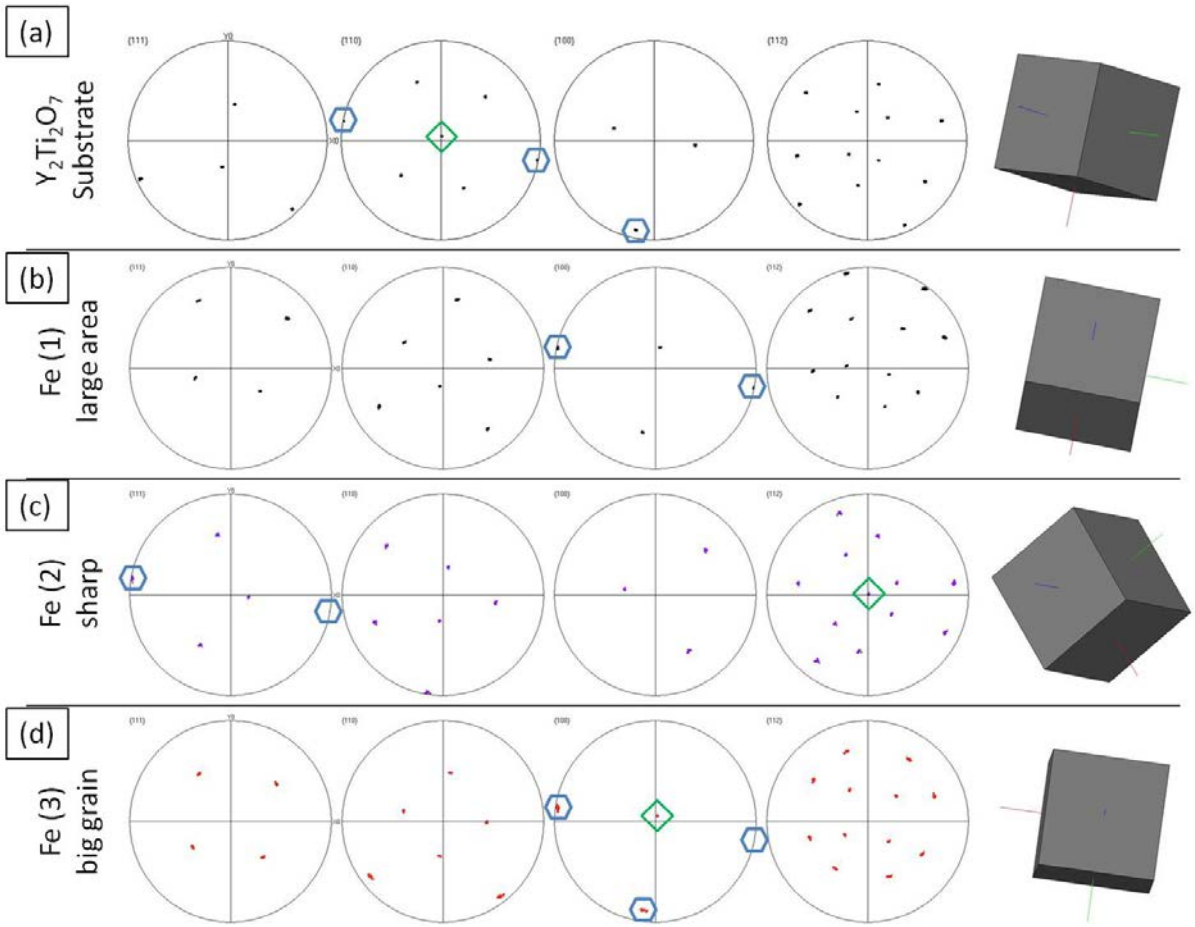

Figure 2. EBSD pole figures from the $Y_2Ti_2O_7$ substrate (a) and from the three types of Fe grains (b – d). Green diamonds show surface orientations while blue hexagons show in-plane orientations. The cubes next to the pole figures represent the full 3D orientation.

Continuing and Future Research

This work is continuing and will be extended to other oxide surface orientations and different deposition conditions. Scanning transmission electron microscopy (STEM) was done on two of the ORs found from

the Fe-{110}YTO samples and the results are still being analyzed. It is not yet known what experimental parameters affect the orientation of the Fe film. Ideally, future samples will contain the same interfacial ORs as those found in the embedded NFs. Furthermore, the CrystalMaker software is being used to analyze the three types of interfaces found in the Fe-{110}YTO sample. Perhaps the three ORs have similar atomic matching. There will also be studies of the interface interactions with irradiation induced defects and He.

Acknowledgements

The authors acknowledge the contributions of Gareth Seward, Mark Cornish, Deryck Stave, and Stephan Kraemer for help with various parts of the research. The work performed at UCSB was supported by the U. S. Department of Energy, Office of Fusion Energy Sciences, under grant DE-FG03-94ER54275.

REFERENCES

[1] G.R. Odette, M.J. Alinger, B.D. Wirth, Annu. Rev. Matter. Res. 38 (2008) 471.
[2] Y. Dai, G.R. Odette, T. Yamamoto, Comp. Nucl. Mater., 1 Chap. 6 (2012) 141.
[3] H. Sakasegawa, L. Chaffron, F. Legendre, et al. J. Nucl. Mater. (2009) 384.
[4] S. Yamashita, S. Ohtsuka, N. Akasaka, et al. Phil. Mag. Lett. (2004) 84.
[5] S. Yamashita, N. Akasaka, S. Ohnuki, J. Nucl. Mater. (2004) 329.
[6] M. Klimiankou, R. Lindau, A. Möslang, J. Nucl Mater (2004) 329.
[7] M. Klimiankou, R. Lindau, A. Möslang, Micron (2005) 36.
[8] T. Okuda, M. Fujiwara, J. Mater. Sci. Lett. (1995) 14.
[9] Y. Wu, E.M. Haney, N.J. Cunningham, et al., Acta Mater. 60 (2012) 3456.
[10] J. Ribis, Y. de Carlan, Acta Mater. 60 (2012) 238.
[11] J. Ciston, Y. Wu, G. R. Odette, et al., Fus. Mat. Semiann. Prog. Rep. (2012) DOE-ER-0313/51.
[12] T. Stan, Y. Wu, G.R. Odette. et al., Metal. and Mater. Trans. A, 44 (2013) 10.
[13] Fusion Semiannual Report, DOE/ER 0313/54, 7.3.